Available online at www.sciencedirect.com
ScienceDirect
Thermochimica Acta 460 (2007) 44–49
thermochimica acta
www.elsevier.com/locate/tca

Catalytic effect of zinc oxide on the reduction of barium sulfate by methane

R. Alizadeh[*], E. Jamshidi, H. Ale Ebrahim

Department of Chemical Engineering, Center of Petrochemical Excellency, Amirkabir University of Technology (Tehran Polytechnic), Tehran 15875-4413, Iran

Received 28 December 2006; received in revised form 29 April 2007; accepted 3 May 2007
Available online 7 May 2007

Abstract

Reduction of barium sulfate by methane was investigated in this work. The thermogravimetric method was used to obtain kinetic parameters of the reaction in the temperature range of 900–975 °C at atmospheric pressure. The kinetics of the reaction has been studied both in the absence and presence of zinc oxide as a catalyst. The conversion–time data have been interpreted by using the grain model, and the effect of catalyst on the kinetic parameters has been elucidated. It was found that zinc oxide acted as fairly strong catalyst for the reaction, especially at higher temperatures. At about 975 °C the reaction rate constant was increased more than 7 times by using 2% of zinc oxide. This enhancement in the rate constant is valuable for industries.

Keywords: Barium sulfate; Reduction; Methane; Catalyst; Kinetic study

1. Introduction

Reduction of barium sulfate ($BaSO_4$) to barium sulfide (BaS) is an important step for the producing of barium chemicals from barite (natural barium sulfate mineral). Barite ore is a basic starting material for manufacturing of a variety of barium chemicals such as $BaCO_3$, $Ba(OH)_2$, $Ba(NO_3)_2$, $Ba(HS)_2$, BaO, etc. In the so-called “black-ash process”, the reduction of barite is carried out in a rotary kiln or in a fluidized bed at a high temperature such 1100–1200 °C in the presence of reducing agents, mostly coal [1].

In the course of reduction, the prime reducing agent is carbon monoxide, which in turn, is generated in situ by the reduction of carbon dioxide by carbon [2].

Studies on the kinetics of the reduction of barite have been very limited. Only a few Russian scientists have carried out mechanistic studies of the reduction of barite by carbon [3–5]. Then Lozhkin et al. have studied the kinetics of barite reduction by carbon [6]. Pelovski et al. [7] studied reduction of barium sulfate by carbon in the presence of some inorganic soluble salts like sodium carbonate, sodium chloride and calcium chloride. They observed that these additives act as promoters for the reduction process. Hargreaves and Murray studied the reduction of pure barium sulfate and barite to barium sulfide in an indirectly heated tube furnace using carbon as the reducing agent and elucidated the factors influencing reduction rate [8]. Jagtap et al. studied reduction of high-grade barite powder with active charcoal both in the absence and presence of catalysts such as Na_2CO_3 and $Fe(NO_3)_3$ [2]. They found that the reaction rate constant was increased 2.75 times by using 5% of Na_2CO_3 and 1.8 times by using 5% of $Fe(NO_3)_3$ at 950 °C. Recently, Gokarn et al. studied the non-isothermal carbothermic reduction of barite in the absence and presence of Sodium vanadate catalyst [9]. All studies are unanimous of the opinion that initial reduction of barite with carbon takes place according to the following equation:

$$BaSO_4 + 4C \rightarrow BaS + 4CO \qquad (1)$$

where both barite and carbon are in contact. The CO generated diffuses and reacts with barite, which is not in contact with carbon, as follows:

$$BaSO_4 + 4CO \rightarrow BaS + 4CO_2 \qquad (2)$$

---

[*] Corresponding author. Present address: School of Material Science and Engineering, University of New South Wales, Sydney 2052, Australia.
Tel.: +61 2 9385 4439; fax: +61 2 9385 5956.
E-mail address: r.alizadeh@cic.aut.ac.ir (R. Alizadeh).

0040-6031/$ – see front matter © 2007 Elsevier B.V. All rights reserved.
doi:10.1016/j.tca.2007.05.006

This CO_2 diffuses back into carbon to generate more CO according to the Boudouard reaction:

$$C + CO_2 \rightarrow 2CO \quad (3)$$

Thus, in the solid-state reduction of barite, CO is the gaseous intermediate. Also Pelovski et al. have studied the isothermal reduction of barite with hydrogen; in this study the kinetic parameters of reaction were determined [10]. Newly Sohn et al. have studied the isothermal reduction of barium sulfate with hydrogen in the presence and absence of nickel catalyst; in this study the kinetic parameters of the reaction were determined [11,12]. The reduction of inorganic mineral with coal is not environmentally friendly. These reactions produce poisonous gases such as SO_2, CO and large amount of CO_2. But reduction of these minerals with methane produces less CO_2 and not any SO_2 and CO.

There are some countries in the world (such as Iran) where coal is not abundant but large sources of natural gas are available, therefore using methane or natural gas for the ore reduction process in these countries will be economically beneficial and favorable [13].

There is not any experimental study on the barium sulfate reduction by methane in the literature. Thus, it is essential to study such reduction process and estimate kinetic parameters for designing industrial plants. It is the goal of the present investigation to study the reduction of the barite by methane and propose a kinetic model, both in the presence and absence of zinc oxide as a catalyst.

2. Thermodynamic considerations

Common method for the barite reduction is based on high temperature reaction with coke. The enthalpy change and the overall reaction are as follows:

$$BaSO_4 + 4C \rightarrow BaS + 4CO, \quad \Delta H^{\circ}_{rx} = 123\,\text{kcal/gmole} \quad (4)$$

where ΔH°_{rx} is the heat of reaction.

Methane is a strong reducing agent, and can react at lower temperature simply:

$$BaSO_4 + CH_4 \Leftrightarrow BaS + CO_2 + 2H_2O, \quad \Delta H^{\circ}_{rx} = 47\,\text{kcal/gmole} \quad (5)$$

Consider a general equation, as follows:

$$\upsilon_R R \Leftrightarrow \upsilon_P P \quad (6)$$

where R and P are the reactants and products, and υ_R and υ_P are the stoichimetric coefficients of reactants and products, respectively.

The equilibrium constant of this reaction can be calculated from the following equation [14]:

$$\log K = \sum \upsilon_P \log K_{f,P} - \sum \upsilon_R \log K_{f,R} \quad (7)$$

where K is the equilibrium constant of the reaction and $K_{f,R}$ and $K_{f,P}$ are equilibrium constant for the formation of reactants and products, respectively. From these equations the equilibrium constants of the reactions computed, and are tabulated in Table 1. Where K_{CO} and K_{CH_4} are the equilibrium constant for the reactions in Eqs. (2) and (5), respectively. From Table 1, the greater reducing power of methane contrast with the carbon monoxide can be seen. Therefore, the operating temperature can be decreased from about 1200 °C (black-ash process) to about 950 °C for this process. This new process of barite reduction with methane has been registered as a patent [15].

Table 1
Equilibrium constants for reaction according to Eqs. (5) and (2)

T (°C)	K_{CH_4}	K_{CO}
800	92×10^6	2,029
900	490×10^6	164,816
1000	3054×10^6	75,683

3. Experimental setup

The thermogravimetric method was used to determine the kinetic parameters of the reaction; this method was explained comprehensively in elsewhere [16]. The experimental setup is shown in Fig. 1. The vertical type high capacity thermogravimeter (model TGH-1500) has been used from Rheometric Scientific. The pellets were made using pure barium sulfate powder, and then were placed inside a platinum basket suspended from a string of a balance with an accuracy of 3 μg. The system was heated to the desired temperature under an inert gas stream such as helium or nitrogen (gas 1 line). Then the isothermal period begins and after temperature stabilization, reducing gas (a mixture of CH_4/He through gas 2 line) is introduced from the bottom of the TG. The outlet gas stream leaves the system from the top and through a bubbler (for slight positive pressure control).

The mole fraction of methane in the input gas mixture was fixed about 0.4. The barium sulfate ($BaSO_4$) powder was used from Merck (Art. No. 1750) with a mean particle size of 0.22 μm. Also zinc oxide (ZnO) powder was used from Merck

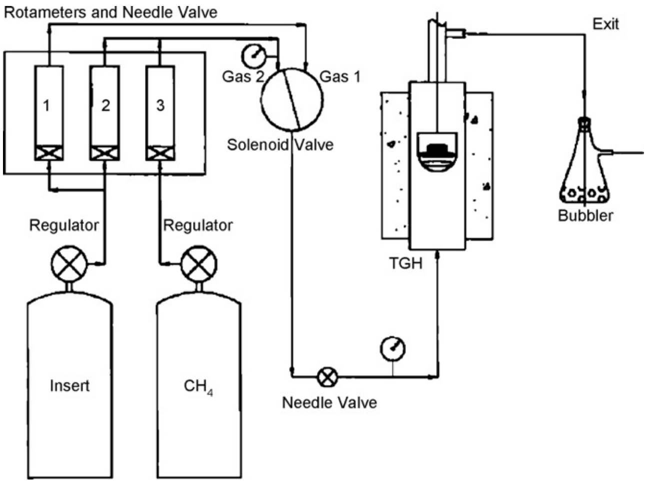

Fig. 1. Flow diagram of system for kinetic study of this reaction.

(Art. No. 8849) with a mean particle size of 0.23 μm. The sizes of particles were calculated by using the average specific surface area of pellet that measured by BET analysis. Methane from Air Products Company with 99.95% purity, helium and nitrogen with 99.999% purity from Messer Griesheim and Air Products Companies are used.

Barium sulfate pellets were made by mechanical pressing of the powder in a pressing mold (3000 kg/cm^2). The diameter and height of the pellets are about 7.2 and 0.6 mm, respectively. Therefore, the pellets can be assumed as slablike. The reduction experiments were carried out in the temperature range of 900–975 °C under atmospheric pressure. Experiments were carried out under the excessive reducing gas condition that the reaction rate is not affected by the gas flow rate. Therefore, the external mass transfer resistance was negligible during the reaction. Two series of experiments were carried out. In the first series of experiments, pure pellets of barium sulfate were used. In the second series, the catalytic effect of zinc oxide on the reduction of barium sulfate was elucidated.

4. Results discussion

Because zinc oxide was found to substantially enhance the rate of the methane reduction of lead oxide [17], its effect on the reduction of barium sulfate was determined in this work.

The transient weight loss of the barium sulfate pellet versus time in the thermogravimeter during the reaction was shown in Fig. 2 at the temperature of 975 °C and methane concentration of 0.4-mole fraction. Also the isothermal X (conversion) versus time curves are shown in Figs. 3–6 for four different temperatures 900, 925, 950 and 975 °C.

The substantial effect of catalyst on barium sulfate reduction can be seen from the thermogravimeric curve as well as the conversion–time plots.

The reaction rate constants can be calculated for different temperatures using procedure presented in Appendices A and B. The numerical values of the reaction rate constantans at different temperature and for three typical cases (with 1% and 2% catalyst and noncatalytic) are presented in Table 2. By compar-

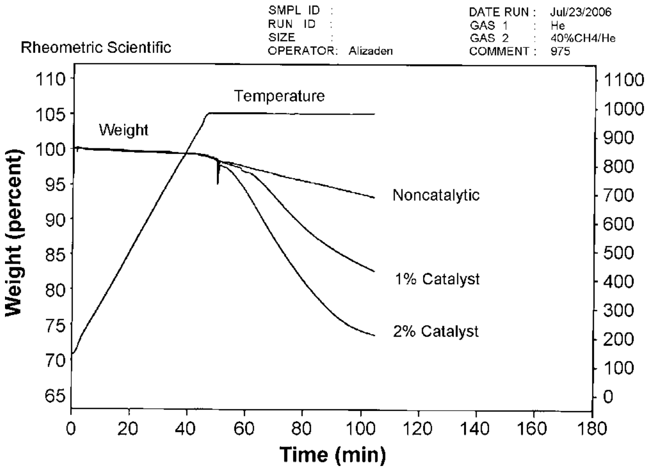

Fig. 2. Weight change curve at $T = 975\,^{\circ}\mathrm{C}$ vs. time.

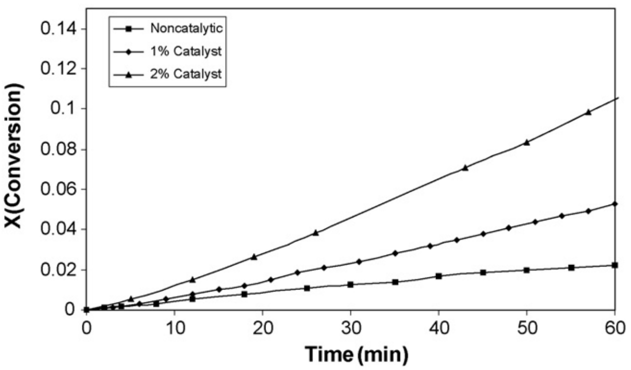

Fig. 3. Effect of catalyst on the isothermal reduction of barium sulfate at $T = 900\,^{\circ}\mathrm{C}$.

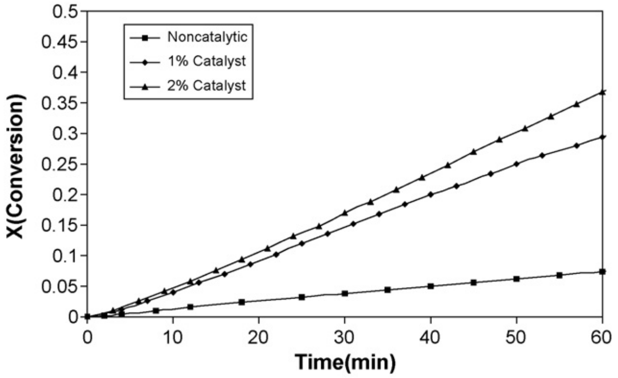

Fig. 4. Effect of catalyst on the isothermal reduction of barium sulfate at $T = 925\,^{\circ}\mathrm{C}$.

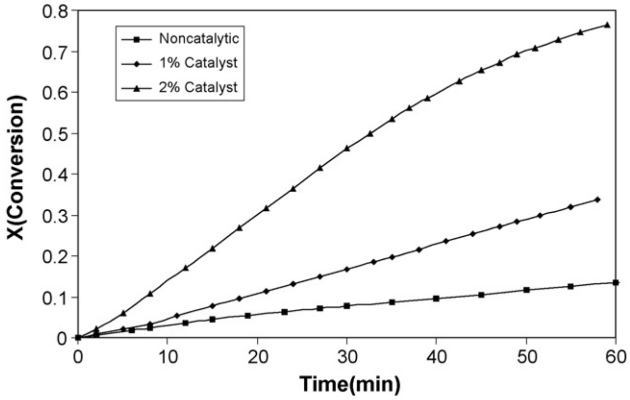

Fig. 5. Effect of catalyst on the isothermal reduction of barium sulfate at $T = 950\,^{\circ}\mathrm{C}$.

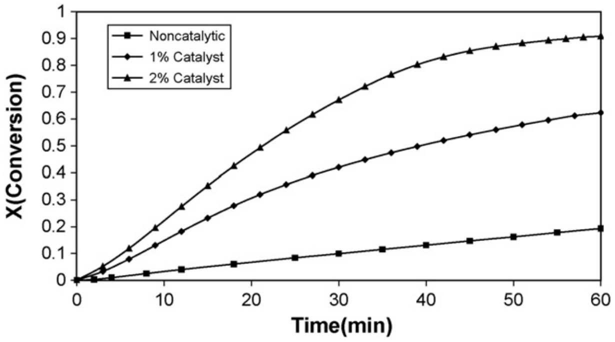

Fig. 6. Effect of catalyst on the isothermal reduction of barium sulfate at $T = 975\,^{\circ}\mathrm{C}$.

Table 2
Rate constants (k (cm/s)) for the reduction of barium sulfate by methane under catalytic and noncatalytic condition

T (°C)	Noncatalytic	1% catalyst	2% catalyst
900	1.108×10^{-7}	2.84×10^{-7}	5.97×10^{-7}
925	3.395×10^{-7}	1.42×10^{-6}	2.03×10^{-6}
950	5.49×10^{-7}	1.8×10^{-6}	4.68×10^{-6}
975	9.44×10^{-7}	5.36×10^{-6}	7.24×10^{-6}

ing the results in Table 2, it seen that zinc oxide has considerable influence in enhancing the value of k and hence the reactivity of methane with $BaSO_4$. Like as the reduction of lead oxide (PbO) with methane [17], this effect may be due to the reduction of zinc oxide by methane as a following reaction [18]:

$$ZnO + CH_4 \rightarrow Zn + CO + 2H_2 \quad (8)$$

All of produced gases by this reaction are reducing agent and can react in situ with barium sulfate and cause the following reactions simultaneously [9,11,19]:

$$BaSO_4 + 4CO \rightarrow BaS + 4CO_2 \quad (2')$$

$$BaSO_4 + 4H_2 \rightarrow BaS + 4H_2O \quad (9)$$

$$BaSO_4 + 4Zn \rightarrow BaS + 4ZnO \quad (10)$$

Furthermore, pore development in solid matrix due to zinc volatility increase the reaction surface area. Also zinc oxide plays a beneficial role of increasing the number of active sites generated in barium sulfate matrix.

The reduction process starts with adsorption of methane on the active sites of the oxide surface and its decomposition, described by the following reactions [20]:

$$CH_4(gas) \rightleftharpoons CH_4(ad) \quad (11)$$

$$CH_4(ad) \rightleftharpoons CH_3(ad) + H(ad) \quad (12)$$

$$CH_3(ad) \rightleftharpoons CH_2(ad) + H(ad) \quad (13)$$

$$CH_2(ad) \rightleftharpoons CH(ad) + H(ad) \quad (14)$$

$$CH(ad) \rightleftharpoons C(ad) + H(ad) \quad (15)$$

$$2H(ad) \rightleftharpoons H_2(gas) \quad (16)$$

The overall reaction of methane adsorption and cracking may be presented as:

$$CH_4 \rightarrow \cdots \rightarrow C_{ad} + 2H_2 \quad (17)$$

In which C_{ad} represents active carbon species adsorbed on solid surface, and is substantially different from deposited solid carbon.

Fig. 7 shows the X-ray diffraction pattern of the product of the completely reduced of barium sulfate with 2% of zinc oxide using methane at a temperature 950 °C. Only barium sulfide was detected by XRD. The zinc or zinc oxide is not seen in the XRD pattern also there is not seen any carbide or oxide phase. It was assured that when barium sulfate is reacted with methane, the solid product is barium sulfide.

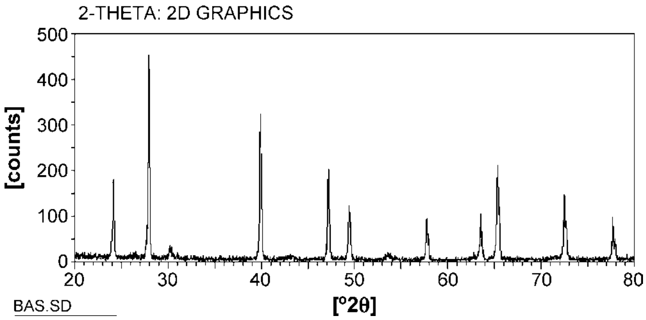

Fig. 7. XRD pattern of BaS produced at $T = 950$ °C and catalysed by 2% of zinc oxide.

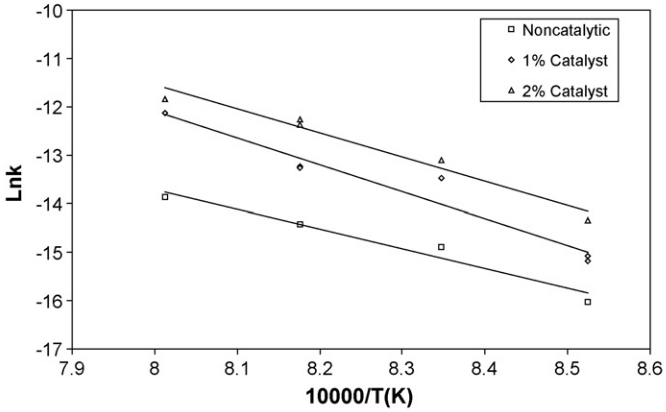

Fig. 8. Arehenius plot for the reaction rate constants in three modes.

The Arrhenius equation is obtained by considering temperature effect on the reaction rate as follows:

$$k = k' \, e^{-E_a/R_g T} \quad (18)$$

where k' is the frequency factor and E_a is the apparent activation energy. Arrehenius plots for three aforementioned modes are shown in Fig. 8.

From Eq. (18) the average activation energy of the barium sulfate reduction is found to be about 96 kcal/gmole. It is useful to make comparisons with activation energy data for other compounds reduction reactions by methane given in the literature; for example, the activation energy for reduction of ZnO to Zn with methane in the temperature range of 840–930 °C is found to be 67.09 kcal/gmole [18], also, the activation energy for reduction of Fe_2O_3 to Fe with methane is 52.7 kcal/gmole in the temperature range of 875–950 °C [21], finally activation energy for reduction of cobalt oxide with methane has been found to be 37 kcal/gmole in the temperature range of 800–950 °C [22]. Thus, the value reported in this article for reduction of barium sulfate with methane is within the same order of magnitude for reduction of ZnO, Fe_2O_3 and CoO with methane.

5. Conclusions

The reduction of barium sulfate with methane was studied in this work. Solid barium sulfide was formed as a product of reaction. The kinetic parameters of this reaction were calculated in presence and absence of catalyst at temperature range of 900–975 °C. This reaction temperature is 200 °C lower than the temperature of reduction with coal (black-ash process).

It was found that zinc oxide acted as fairly strong catalyst for the reaction, especially at higher temperature. Fig. 5 shows 250% and 600% increase in conversion with 1% and 2% catalyst at temperature 950 °C, respectively. Fig. 6 shows 300 percent and 450 percent increase in conversion with 1% and 2% catalyst at temperature 975 °C, respectively. By using the Grain model, the rate constants of reaction calculated and tabulated in Table 2. This calculation shows that the rate constant increases from 9.44×10^{-7} to 72.4×10^{-7} cm/s at temperature 975 °C. The reaction of barium sulfate with methane is environmentally friendly. This new method for barite reduction can be a good application for natural gas [15]. This method reduces greenhouse gas emission (CO_2) up to 70%, and does not produce any SO_2, CO and fly ash as black-ash process.

Appendix A

The chemical reaction under consideration is expressed by Eq. (5) as follow:

$$BaSO_4 + CH_4 \rightarrow BaS + CO_2 + 2H_2O \tag{A.1}$$

The "conversion" is defined as the weight loss of a pellet at a given time divided by the pellet weight when it is completely reduced, i.e., all the oxygen atoms are liberated from it. Thus, the conversion–time curves can be obtained from the Thermogravimeter curves using the following relation:

$$X(t) = \frac{W_0 - W(t)}{W_0(M_{O_4}/M_{BaSO_4})} = 3.64\left(1 - \frac{W(t)}{W_0}\right) \tag{A.2}$$

where $W(t)$ is the measured weight at time t; W_0 the initial pellet weight; M_{O_4} and M_{BaSO_4} are the molecular weights of liberated oxygen and barium sulfate, respectively.

The grain model introduced by Szekely et al. was used to analyze experimental data. This model is well described in the literature and only a brief development is offered here [23].

The barium sulfate–methane reaction may be represented by the following equation:

$$A_{(gas)} + bB_{(solid)} \rightarrow cC_{(gas)} + dD_{(solid)} \tag{A.3}$$

where b and d are the stoichiometric coefficient of the solid reactant B and solid product D, respectively and c is the stoichiometric coefficient of the product gas. The modeling is based upon the following assumption:

(1) The pellet retains its initial size throughout the reaction.
(2) The reaction system is isothermal.
(3) The external mass transfer resistance is negligible.
(4) The intrinsic reaction rate is irreversible and first order with respect to methane concentration.
(5) The pseudo-steady approximation is valid.

The solid reactant is visualized as being composed of a large number of highly dense, spherical grains, each of these grain reacts individually according to unreacted shrinking core model. In the overall pellet, however, the reaction occurs in a zone rather than at a sharply defined boundary. Reactant gas undergoes mass transfer from the bulk gas stream to pellet surface. From the surface the gas must diffuse to arrive at a sharp interface between the grain particle and the product layer for reaction to take place.

The dimensionless governing equations of grain model for slablike pellet with spherical grains are as follows [24]:

$$\frac{\partial^2 a}{\partial y^2} = \sigma^2 a (r^*)^2 \tag{A.4}$$

$$\frac{\partial r^*}{\partial \theta_g} = -a \tag{A.5}$$

With the initial and boundary conditions:

$$\theta_g = 0, \quad r^* = 1 \tag{A.6}$$

$$y = 0, \quad \frac{\partial a}{\partial y} = 0 \tag{A.7}$$

$$y = 1, \quad a = 1 \tag{A.8}$$

where $a = C_A/C_{Ab}$ is dimensionless gas concentration that C_A and C_{Ab} are pellet and bulk reactant gas concentrations, respectively. $y = 2z/L_0$ is the dimensionless position in the pellet that z is distance of each point from center of the pellet and L_0 is the initial thickness of the slab pellet. $r^* = r_{g_c}/r_{g_0}$ is the dimensionless unreacted radius in the grain that r_{g_0} and r_{g_c} are initial and unreacted core radius of grain, respectively. θ_g is dimensionless time for grain model defined as follow:

$$\theta_g = \frac{bkC_{Ab}t}{\rho_B r_{g_0}} \tag{A.9}$$

where k is the reaction rate constant, t the time and ρ_B is the true molar density of solid reactant B. σ is the gas–solid reaction modulus, by ignoring structural changes of the pellet, this modulus is defined for flat pellet that made from spherical grains as follow:

$$\sigma = \frac{L_0}{2}\sqrt{\frac{3(1-\varepsilon_0)k}{D_{eA} r_{g_0}}} \tag{A.10}$$

where ε_0 is the pellet porosity and can be estimated using calculation of the pellet volume and measuring the weight of pellet, and D_{eA} is the effective diffusion coefficient of gaseous reactant in the pellet. D_{eA} was estimated using the random pore model [25]:

$$D_{eA} = D_A \varepsilon_0^2 \tag{A.11}$$

where D_A was determined by combining molecular and Knudsen diffusion coefficients as follows:

$$\frac{1}{D_A} = \frac{1}{D_{AM}} + \frac{1}{D_{AK}} \tag{A.12}$$

where D_{AM} and D_{AK} are molecular and Knudsen diffusivity of gaseous reactant A in the pellet, respectively. D_{AM} was evaluated using the Chapman–Enskog formula [26] and the D_{AK} was calculated from the following equation [23]:

$$D_{\mathrm{AK}} = \frac{4}{3}\left(\frac{8R_{\mathrm{g}}T}{\pi M_{\mathrm{A}}}\right)^{1/2} k_0 \tag{A.13}$$

where R_{g} is the gas constant, T the absolute temperature, M_{A} the molecular weight of gaseous reactant and k_0 was calculated from the 'dusty gas model' of Mason et al. [27] as follows:

$$\frac{1}{k_0} = \left(\frac{128}{9}\right) n_{\mathrm{d}} r_{\mathrm{g}}^2 \left(1 + \frac{\pi}{8}\right) \tag{A.14}$$

n_{d} is the number of solid grains per unit volume of porous solid, was calculated as follows:

$$n_{\mathrm{d}} = \frac{3(1-\varepsilon_0)}{4\pi r_{\mathrm{g}}^3} \tag{A.15}$$

Appendix B

By using above equation, the governing equations can be solved and r^* was found in the time near zero as follows:

$$r^* = 1 - \frac{\cosh(\sigma y)}{\cosh(\sigma)}\theta_{\mathrm{g}} \tag{B.1}$$

Extent of reaction or conversion for non-porous grains is defined as local conversion and is the ratio of mass of solid product produced at each time to mass of solid product if the grain converts to solid product completely; so for grains we have:

$$x = 1 - (r^*)^{F_{\mathrm{g}}} \tag{B.2}$$

where x is the local conversion of the grains and F_{g} is the grain shape factor, which equals as 1, 2 and 3 for slablike, cylindrical and spherical grains, respectively. However, conversion of pellet (X) is defined as overall conversion and is calculated from local conversion integration over the pellet as follows:

$$X = \int_0^1 x\,\mathrm{d}y = 1 - \int_0^1 (r^*)^3\,\mathrm{d}y \tag{B.3}$$

If the Eq. (B.1) was combined with Eq. (B.3) and then integrated, the conversion of pellet could be found at the time near zero. Then the slope of conversion–time curve in the vicinity of the zero can be shown to be as follows:

$$\left.\frac{\mathrm{d}X}{\mathrm{d}t}\right|_{t=0} = \frac{3bkC_{\mathrm{Ab}}}{\rho_{\mathrm{B}} r_{\mathrm{g}_0}} \frac{\tanh(\sigma)}{\sigma} \tag{B.4}$$

References

[1] Kirk-Othmer, Encyclopedia of Chemical Technology, vol. 3, Wiley, New York, 1991, pp. 902–931.
[2] S.B. Jagtap, A.R. Pande, A.N. Gokarn, Ind. Eng. Chem. Res. 29 (1990) 795–799.
[3] V.A. Shushunov, G.I. Sadovnikov, B.Y. Andrew, Zh. Fiz. Khim. 28 (1954) 1472–1478.
[4] V.V. Pechkovski, A.N. Ketov, Zh. Prkl. Khim. 33 (1960) 1719–1723.
[5] A.A. Ravdel, N.A. Novikova, J. Appl. Chem. USSR 36 (1963) 1384–1392.
[6] A.F. Lozhkin, V.A. Pashcenko, F.V. Povar, J. Appl. Chem. USSR 47 (1974) 1031–1034.
[7] Y. Pelovski, I. Gruchavov, I. Dombalov, J. Therm. Anal. 32 (1987) 1743–1745.
[8] K. Hargreaves, D.M. Murray, J. Chem. Technol. Biotechnol. 45 (1989) 319–325.
[9] A.N. Gokarn, S.D. Pradhan, G. Pathak, S.S. Kulkarni, Fuel 79 (2000) 821–827.
[10] Y. Pelovski, K. Ninova, I. Gruchavov, I. Dombalov, J. Therm. Anal. 36 (1990) 2037–2043.
[11] H.Y. Sohn, M. Savic, R. Padilla, G. Han, Chem. Eng. Sci. 61 (2006) 5082–5087.
[12] H.Y. Sohn, M. Savic, R. Padilla, G. Han, Chem. Eng. Sci. 61 (2006) 5088–5093.
[13] Kirk-Othmer, Encyclopedia of Chemical Technology, vol. 13, Wiley, New York, 1991, p. 745.
[14] I. Brain, Thermochemical Data of Pure Substances, VCH, Weinheim, 1995.
[15] E. Jamshidi, H. Ale Ebrahim, Iranian Patent No. 26,997 (2001).
[16] J.M. Smith, Chemical Engineering Kinetics, McGraw Hill, New York, 1981.
[17] H. Ale Ebrahim, E. Jamshidi, Ind. Eng. Chem. Res. 44 (2005) 495–504.
[18] H. Ale Ebrahim, E. Jamshidi, Trans. Inst. Chem. Eng. 79A (2001) 62–70.
[19] H. Ale Ebrahim, Ph.D. Thesis, Amirkabir University of Technology, Tehran, Iran, 1998.
[20] O. Ostrovski, G. Zhang, AIChe J. 52 (2006) 300–310.
[21] D. Ghosh, A.K. Roy, A. Ghosh, Trans. ISIJ 26 (1986) 186–193.
[22] B. Khoshandam, R.V. Kumar, E. Jamshidi, Metall. Mater. Trans. 35B (2004) 825–828.
[23] J. Szekely, J.W. Evans, H.Y. Sohn, Gas–Solid Reactions, Academic Press, New York, 1976.
[24] H.Y. Sohn, J. Szekely, Chem. Eng. Sci. 27 (1972) 763–778.
[25] N. Wakao, J.M. Smith, Chem. Eng. Sci. 17 (1962) 825–834.
[26] R.B. Bird, W.E. Stewart, E.N. Lightfoot, Transport Phenomena, first ed., Wiley, New York, 1960.
[27] E.A. Mason, A.P. Malinauskas, R.B. Evans, J. Chem. Phys. 46 (1976) 3199–3216.